Microgrid Stability Improvement by Optimization of Virtual Droop Control

Binu Krishnan U
Research Scholar
Department of Electrical Engineering
NIT Calicut, Kerala
binukrishnanu13@gmail.com

Mija S J
Assistant Professor
Department of Electrical Engineering
NIT Calicut, Kerala
mija@nitc.ac.in

Elizabeth P Cheriyan
Associate Professor
Department of Electrical Engineering
NIT Calicut, Kerala
epc@nitc.ac.in

***Abstract*—The concept of microgrid has become more relevant due to the increase in the use of distributed energy resources. However, the important factors which are to be considered are their ability to control the power flow and stability of the system. Droop control strategy requires no communication system and realizes the "plug and play" function between source and load. Virtual impedance type droop control method is preferred to improve the transient response and power decoupling of conventional droop method. In this paper a state space model of such a system is developed based on small signal disturbances. Eigenvalue analysis of the system is also done and the parameters which determine the stability of the system are identified. The optimum values of these parameters are found out by increasing the stability of the system using particle swarm optimization (PSO) technique. The simulation is done by MATLAB coding and the results show that the values of the optimized parameters will improve the stability of the system by shifting the eigenvalues away from the imaginary axis as far as possible on the left half of s plane.**

Keywords—Droop controller; microgrid; eigenvalue analysis; particle swarm optimization

I. INTRODUCTION

The concept of distribution generation is highly promoted and become more relevant due to environmental considerations and as an alternative to fossil fuels [1], [2]. The generation which are not centrally dispatched and controlled can be considered as distribution generation which is usually connected to the distribution part of the power system. The development of distributed generation leads to the concept of microgrid [3]. The multiple distributed resources in a microgrid operates in parallel and power converters associated will have different control objectives as in [4]-[6].

Different control strategies like multi agent control, master slave control and droop control are proposed in the literature [7], [8]. Among these, the droop control method has been identified as the popular method for controlling the operation of different DG units within the microgrid. The droop control method mimics the operation of conventional droop characteristics of alternator in which real and reactive power sharing is done by varying the magnitude of operating voltage and frequency. The significance to know the response of the system to various disturbances leads to the widespread use of small signal model [9], [10].

The inductance to resistance ratio of DG systems is usually low and because of that, there exist a coupling between active and reactive power when droop based control is used. Another problem with droop control method is its poor transient response. In order to compensate these limitations, virtual impedance is introduced in the control system of each DG unit. In this paper, a detailed model of inverter based microgrid is presented. Each DG inverter will have an outer power control loop based on droop control and inner voltage and current control loop. A small-signal state-space model is constructed on a synchronous reference frame whose rotation frequency is set by the power controller of individual inverter as in [11].

The analysis of eigenvalues can be done after obtaining the state space model of the microgrid from which the stability and dynamic performance is analyzed. The variation of eigenvalues with respect to the variation of different parameters in the control loops is also analyzed. After identifying the main parameters which will affect the stability and performance, these parameters are optimized. In [12] parameters are optimized based on the genetic algorithm by minimizing the difference between measured and reference values of active and reactive power in which adequacy is the main control objective. The stability analysis of the system by varying the position of eigenvalue is not done in this method. The feasible range and optimum value of virtual impedance is found out in [13]. But the analysis of the effect of the optimum impedance value on stability is not done. In this paper, the optimization is done by PSO taking the objective function as the minimization of the extreme right eigenvalue and thus stability of the system is improved.

II. MICROGRID SYSTEM

Fig. 1 shows the single-line diagram of the study system. It contains two DGs which are connected to its local loads through inverter, LC filter and coupling inductor. A common load is also connected through a line. When microgrid is operated in the autonomous mode, apart from meeting the load requirement, it has to maintain the voltage and frequency within the allowable limits.

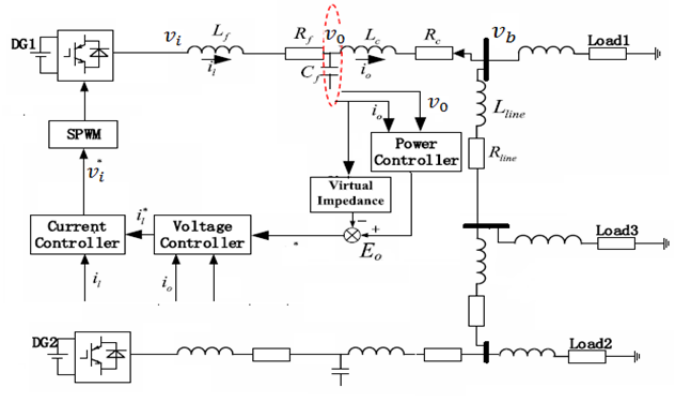

Fig. 1. Microgrid study system.

III. MICROGRID SMALL SIGNAL MODEL

The model presented in this paper consists of three submodules which are inverter model, line model and load model. Each inverter is modeled in its individual reference frame and then transferred into a common reference frame.

A. Inverter Model

The droop controller of a Voltage source inverter consists of power sharing controller, voltage controller and current controller as in Fig. 2.

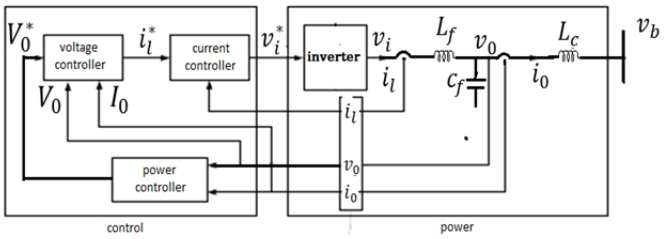

Fig. 2. Inverter model.

The reference values of voltage and frequency are set by the power sharing controller given in Fig. 3 according to the desired values of real and reactive power.

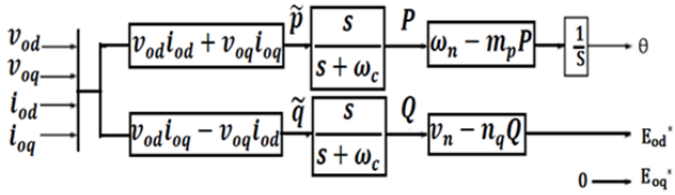

Fig. 3. Power sharing controller.

The corresponding equations are:

$$P = \frac{s}{s+\omega_c}(v_{od}i_{od} + v_{oq}i_{oq}) \quad (1)$$

$$Q = \frac{s}{s+\omega_c}(v_{od}i_{oq} - v_{oq}i_{od}) \quad (2)$$

$$\omega = \omega_n - k_p P, \qquad \dot{\theta}=\omega \quad (3)$$

$$E_{od}{}^* = v_n - k_q Q, \qquad E_{oq}{}^* = 0 \quad (4)$$

$$\theta = \omega_n t + \delta \quad (5)$$

where,

P : Fundamental component of real power,

Q : Fundamental component of reactive power,

v_o :LC filter output voltage,

i_o :LC filter output current,

E_0^* :Reference output voltage of power controller

ω_c :Cut off frequency of Low pass filter,

δ :Angle of inverter reference frame with respect to the common reference frame

The Reference input voltage of voltage controller is obtained by considering the virtual impedance as

$$V_0^* = E_0^* - I_o Z_o = E_0^* - I_o(R_o + jX_o) \quad (6)$$

where,

Z_o :Virtual impedance,

R_o :Virtual resistance,

X_o :Virtual inductance

From equations(3) and (5),

$$\dot{\delta} = -k_p P \quad (7)$$

Linearizing the above equations for small perturbation and rearranging, small signal model of power sharing controller is obtained as

$$\begin{bmatrix}\Delta\dot{\delta}\\ \Delta\dot{P}\\ \Delta\dot{Q}\end{bmatrix} = A_1\begin{bmatrix}\Delta\delta\\ \Delta P\\ \Delta Q\end{bmatrix} + A_2\begin{bmatrix}\Delta i_l\\ \Delta v_o\\ \Delta i_o\end{bmatrix} \quad (8)$$

$$\begin{bmatrix}\Delta\omega\\ \Delta v_0{}^*\end{bmatrix} = \begin{bmatrix}B_1\\ B_2\end{bmatrix}\begin{bmatrix}\Delta\delta\\ \Delta P\\ \Delta Q\end{bmatrix} + B_3\begin{bmatrix}\Delta i_l\\ \Delta v_o\\ \Delta i_o\end{bmatrix} \quad (9)$$

where,

$$\Delta V_0^* = \begin{bmatrix}\Delta V_{od}^*\\ \Delta V_{oq}^*\end{bmatrix}, \Delta V_0 = \begin{bmatrix}\Delta V_{od}\\ \Delta V_{oq}\end{bmatrix}, \Delta I_l = \begin{bmatrix}\Delta I_{ld}\\ \Delta I_{lq}\end{bmatrix}, \Delta I_0 = \begin{bmatrix}\Delta I_{od}\\ \Delta I_{oq}\end{bmatrix}$$

In output voltage control loop, the output voltage is compared with the reference given by the power sharing controller and a feed forward gain is obtained to compensate for output current disturbances and generate the reference current vector as shown in Fig. 4.

Let time derivative of ϕ be defined as

$$\frac{d\phi_d}{dt} = v_{od}^* - v_{od} \quad (10)$$

$$\frac{d\phi_q}{dt} = v_{oq}^* - v_{oq} \quad (11)$$

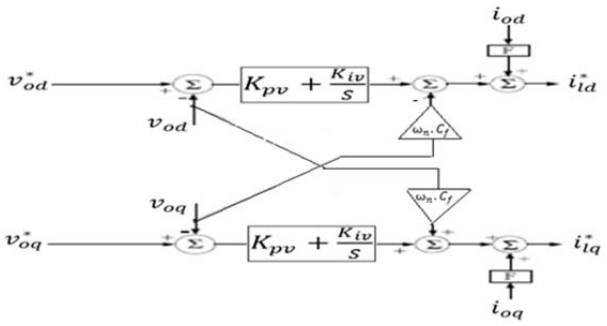

Fig. 4. Voltage controller.

Corresponding state equations are

$$i^*_{ld} = Fi_{od} - \omega_n C_f v_{oq} + K_{pv}(v^*_{od}\text{-}v_{od}) + K_{iv}\phi_d \quad (12)$$

$$i^*_{lq} = Fi_{oq} + \omega_n C_f v_{od} + K_{pv}(v^*_{oq}\text{-}v_{oq}) + K_{iv}\phi_q \quad (13)$$

where,

C_f : filter capacitance

K_{pv} : proportional constant of PI controller

K_{iv} : integral constant of PI controller

Linearizing the above equations, we get

$$\Delta\dot{\phi} = [0][\Delta\phi] + C_1[\Delta V^*_0] + C_2\begin{bmatrix}\Delta i_l\\ \Delta v_o\\ \Delta i_o\end{bmatrix} \quad (14)$$

$$[\Delta i^*_l] = C[\Delta\phi] + C_3[\Delta V^*_0] + C_4\begin{bmatrix}\Delta i_l\\ \Delta v_o\\ \Delta i_o\end{bmatrix} \quad (15)$$

where $\Delta\phi = \begin{bmatrix}\Delta\phi_d\\ \Delta\phi_q\end{bmatrix}$

Similar to voltage controller, current control loop uses a PI controller to compare the output filter current and reference value given by the voltage controller as shown in Fig. 5 and generate reference voltage for the pulse generator.

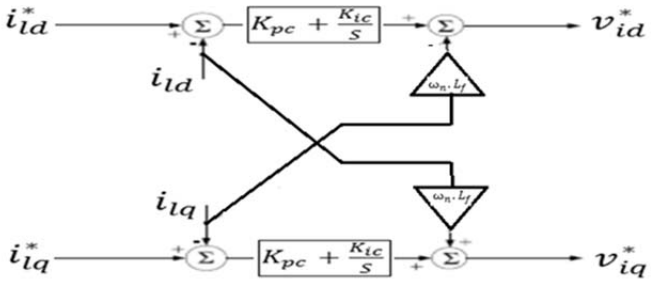

Fig. 5. Current controller.

Let time derivative of γ be defined as

$$\frac{d\gamma_d}{dt} = i^*_{ld}\text{-}i_{ld} \quad (16)$$

$$\frac{d\gamma_q}{dt} = i^*_{lq}\text{-}i_{lq} \quad (17)$$

Corresponding state equations are

$$v^*_{id} = -\omega_n L_f i_{lq} + K_{pc}(i^*_{ld}\text{-}i_{ld}) + K_{ic}\gamma_d \quad (18)$$

$$v^*_{iq} = \omega_n L_f i_{ld} + K_{pc}(i^*_{lq}\text{-}i_{lq}) + K_{ic}\gamma_q \quad (19)$$

where, L_f : filter inductance

K_{pc} : proportional constant of PI controller

K_{ic} : integral constant of PI controller

Linearizing the above equations, we get

$$\Delta\dot{\gamma} = [0][\Delta\gamma] + + D_1[\Delta i^*_l] + D_2\begin{bmatrix}\Delta i_l\\ \Delta v_o\\ \Delta i_o\end{bmatrix} \quad (20)$$

$$[\Delta v^*_i] = D[\Delta\gamma] + D_3[\Delta i^*_l] + D_4\begin{bmatrix}\Delta i_l\\ \Delta v_o\\ \Delta i_o\end{bmatrix} \quad (21)$$

where $\Delta\gamma = \begin{bmatrix}\Delta\gamma_d\\ \Delta\gamma_q\end{bmatrix}$

The voltage and current equations corresponding to the LC filter and coupling inductance can be represented as

$$v_i - v_0 = r_f i_l + L_f\frac{di_l}{dt} \quad (22)$$

$$i_l - i_0 = c_f\frac{dv_0}{dt} \quad (23)$$

$$v_0 - v_b = r_c i_o + L_c\frac{di_o}{dt} \quad (24)$$

where v_b : bus voltage

L_c : coupling inductance

Linearizing and rearranging the above equations after DQ transformation we get,

$$\begin{bmatrix}\Delta\dot{i}_l\\ \Delta\dot{v}_o\\ \Delta\dot{i}_o\end{bmatrix} = \mathrm{E}\begin{bmatrix}\Delta i_l\\ \Delta v_o\\ \Delta i_o\end{bmatrix} + E_1[\Delta v_i] + E_2[\Delta v_{bdq}] + E_3[\Delta\omega] \quad (25)$$

Output variables of each inverter are required to be converted into common reference frame for connecting it to the whole system. Corresponding equations are:

$$i_{OD} = i_{od}cos\delta - i_{oq}sin\delta \quad (26)$$

$$i_{OQ} = i_{od}sin\delta + i_{oq}cos\delta \quad (27)$$

where,

i_{OD}: Direct axis component of current in common reference frame

i_{OQ}: Quadrature axis component of current in common reference frame

Linearizing the above equations, we get

$$[\Delta i_{oDQ}] = T_s[\Delta i_0] + T_c[\Delta\delta] \quad (28)$$

where,

$$T_s = \begin{bmatrix}cos\delta_0 & -sin\delta_0\\ sin\delta_0 & cos\delta_0\end{bmatrix}, T_c = \begin{bmatrix}-I_{od}sin\delta_0 - I_{oq}cos\delta_0\\ I_{od}cos\delta_0 - I_{oq}sin\delta_0\end{bmatrix}$$

Similarly bus voltage on individual inverter reference frame can be represented using reverse transformation as

$$[\Delta v_{bdq}] = [T_s^{-1}]\,[\Delta v_{bDQ}]+[T_v^{-1}]\,[\Delta\delta] \quad (29)$$

where,

$$T_v^{-1}=\begin{bmatrix}-V_{bD}sin\delta_0+V_{bQ}cos\delta_0\\-V_{bD}cos\delta_0-V_{bQ}sin\delta_0\end{bmatrix}$$

V_{bD} is the direct axis component of voltage in common reference frame and $V_{bQ}$is the quadrature axis component of voltage in common reference frame

From (8), (9), (14), (15), (20), (21), (25), (28) and (29):

$$[\Delta\dot{x}_{inv\,i}] = G_{1\,i}\,[\Delta x_{inv\,i}]+G_{2\,i}[\Delta v_{bDQ\,i}] \quad (30)$$

$$\begin{bmatrix}\Delta\omega_i\\\Delta i_{oDQi}\end{bmatrix} = \begin{bmatrix}G_{3\,i}\\G_{4\,i}\end{bmatrix}[\Delta x_{inv\,i}] \quad (31)$$

where,

$$[\Delta x_{inv\,i}] = [\Delta\delta_i \quad \Delta P_i \quad \Delta Q_i \quad \Delta\phi_i \quad \Delta\gamma_i \quad \Delta i_{li} \quad \Delta v_{0i} \quad \Delta i_{oi}]$$

Since there are two inverters in the microgrid system,

$$[\Delta x_{inv}]=[\Delta x_{inv1}\ \Delta x_{inv2}]^T$$

B. Network Model

The voltage difference between adjacent buses j and k as shown in Fig. 6 is given by

$$v_{bj} - v_{bk} = i_{line\,i}r_{line\,i} + L_{line\,i}\frac{di_{line\,i}}{dt} \quad (32)$$

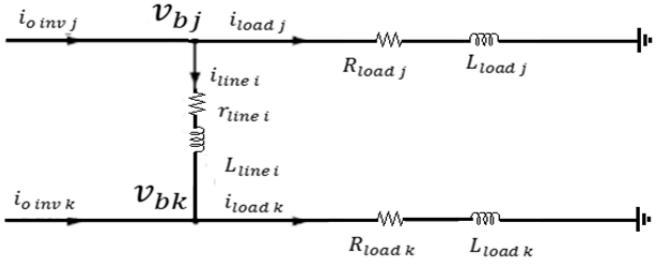

Fig. 6. Network and load model.

Taking DQ transformation and linearization,

$$\Delta\dot{\imath}_{line\,i}=H_{1\,i}[\Delta i_{line\,i}]+H_{2\,i}[\Delta v_{bDQ\,i}]+H_{3\,i}\Delta\omega \quad (33)$$

For given network with 2 lines and 3 nodes, equation become,

$$\Delta\dot{\imath}_{line} =H_1\,[\Delta i_{line}]+H_2\,[\Delta v_{bDQ}]+H_3\,\Delta\omega \quad (34)$$

where,

$$[\Delta i_{line}]=[\Delta i_{line1}\Delta i_{line2}]^T$$

$$[\Delta v_{bDQ}]=[\Delta v_{bDQ1}\Delta v_{bDQ2}\ \Delta v_{bDQ3}]^T$$

C. Load model

Equation of RL load connected at i^{th} node is,

$$v_{bj} = i_{load\,i}R_{load\,i} + L_{load\,i}\frac{di_{load\,i}}{dt} \quad (35)$$

Taking DQ transformation and linearization,

$$\Delta\dot{\imath}_{load}=L_1[\Delta i_{load}]+L_2\,[\Delta v_{bDQ}]+L_3\Delta\omega \quad (36)$$

where $[\Delta i_{load}]=[\Delta i_{load1}\Delta i_{load2}\Delta i_{load3}]^T$

D. Complete microgrid model

Considering the model equations (30), (31), (34) and (36) we get overall state space model as

$$\begin{bmatrix}\Delta\dot{x}_{inv}\\\Delta\dot{\imath}_{line}\\\Delta\dot{\imath}_{load}\end{bmatrix}=A_m\begin{bmatrix}\Delta x_{inv}\\\Delta i_{line}\\\Delta i_{load}\end{bmatrix}+\begin{bmatrix}G_2\\H_2\\L_2\end{bmatrix}[\Delta v_{bDQ}] \quad (37)$$

where, $A_m = \begin{bmatrix}G_1 & 0 & 0\\H_3G_3 & H_1 & 0\\L_3G_3 & 0 & L_1\end{bmatrix}$

To establish the node voltage, a virtual resistor r_N is assumed at each node of the network. Hence, the voltage of i^{th} node is given by

$$V_{b\,i} = r_N(i_{o\,i} - i_{load\,i} + i_{line\,i}) \quad (38)$$

For the selected network with two nodes,

$$[\Delta v_{bDQ}] = R_N(M_1[\Delta i_{\,oDQ}]+ M_2[\Delta i_{\,loadDQ}] + M_3[\Delta i_{\,line}]) \quad (39)$$

where, matrix R_N is of size 6×6, whose diagonal elements are equal to r_N. The matrix M_1 is of size 4×2s, which maps the inverter connection points onto network nodes. Similarly, M_2 of size 6×4 maps load connection points onto the network nodes. Matrix M_3 of size 6×4 maps the connecting lines onto the network nodes.

Based on (37) and (39), 36 order state space model is obtained as

$$\begin{bmatrix}\Delta\dot{x}_{inv}\\\Delta\dot{\imath}_{line}\\\Delta\dot{\imath}_{load}\end{bmatrix}=A_{mg}\begin{bmatrix}\Delta x_{inv}\\\Delta i_{line}\\\Delta i_{load}\end{bmatrix} \quad (40)$$

IV. Eigen Value Analysis

The complete eigenvalue spectrum of the linearized small signal model can be calculated under the initial condition given in Table 1. The parameters of the system are given in Table 2. From the eigenvalue plot shown in Fig. 7, it is observed that the eigenvalues are distributed in three different regions and stability is determined by the low frequency eigenvalues near the imaginary axis.

In order to find out the effect on stability due to the variation of control parameters $k_p, k_q, k_{pv}, k_{pc}, k_{iv}\ k_{ic}, R_0\ and\ X_0$ eigenvalue spectrum is plotted by varying each of these parameters and keeping others constant. From Fig. 8 it can be concluded that as the value of $k_p$increases, the dominant eigenvalues move away from the real axis and closer to the imaginary axis which decreases the stability.

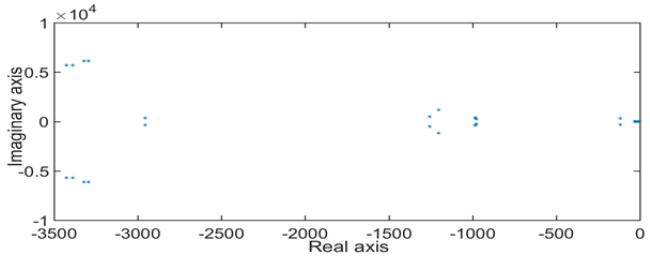

Fig. 7. Eigenvalue spectrum in S plane.

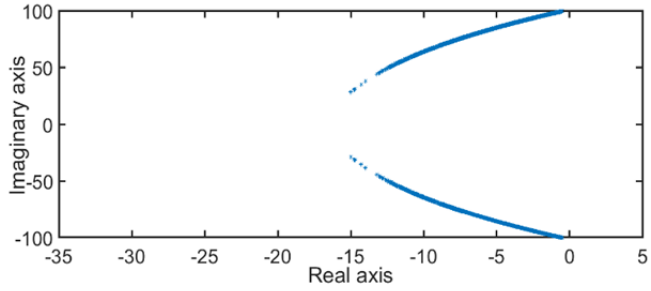

Fig. 8. Variation of eigenvalues with k_p in S plane.

TABLE I. INITIAL OPERATING VALUES

Parameter	Values	Parameter	Values
V_{od}	[311.2 311.6] V	$I_{line\ d1}$	-7.8A
V_{oq}	[0 0]V	$I_{line\ q1}$	1.4A
I_{od}	[21.2 21.2]A	$I_{line\ d2}$	-5.3A
I_{oq}	[-.34 -1.05]A	$I_{line\ q2}$	0.7A
I_{ld}	[21.2 21.2]A	v_{bd}	[308.7 308.5 308]V
I_{lq}	[-14.3 -11.3]A	v_{bq}	[-2.8 -1.3 -1.5]V
δ_0	[-14.3 -11.3]A	ω_0	314rad/s

TABLE II. SYSTEM PARAMETERS OF MICROGRID

Parameter	Values	Parameter	Values
L_f	1.5mH	k_p	1.03 e-5
R_f	0.15Ω	k_q	2.95 e-4
C_f	1500μF	K_{pv}	10.11
L_c	0.15mH	K_{iv}	100
R_c	0.05Ω	K_{pc}	10
R_{line1}	0.147Ω	K_{ic}	0.12
L_{line1}	1.63mH	F	0.7
R_{line2}	0.11Ω	ω_c	31.4rad/s
L_{line2}	1.25mH	R_0	0.05Ω
		X_0	0.2Ω

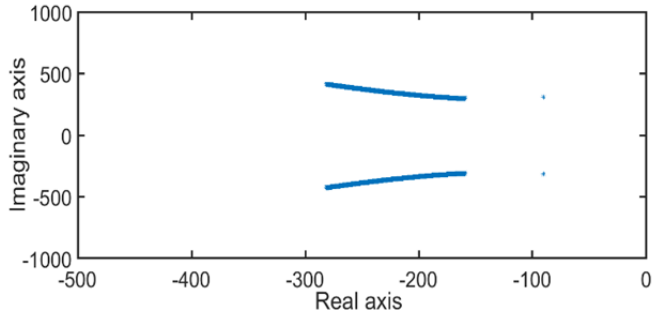

Fig. 9. Variation of eigenvalues with k_q in S plane.

Similarly as k_q increases, dominant eigenvalues move towards unstable region as shown in Fig. 9. Similar variation is obtained when k_{pv}, k_{ic}, R_0 *and* X_0 are changed as shown in Fig. 10 to 13, respectively and the variation is less when k_{pc} *and* k_{iv} are changed. So it can be concluded that the main parameters which determine the stability of the system are k_p, k_q, k_{pv}, k_{ic}, R_0 *and* X_0.

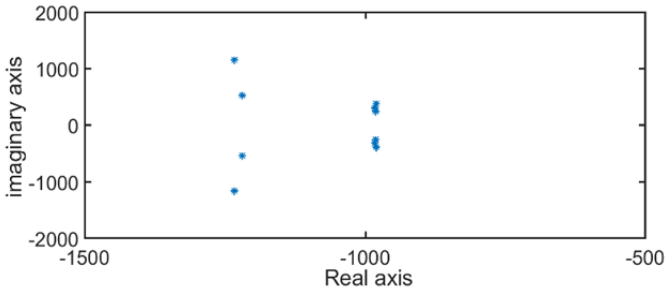

Fig. 10. Variation of eigenvalues with k_{ic} in S plane.

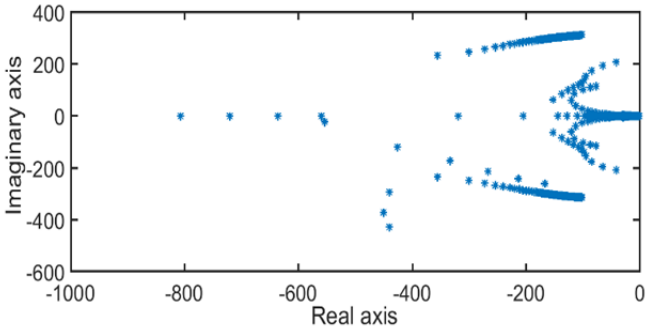

Fig. 11. Variation of eigenvalues with k_{pv} in S plane.

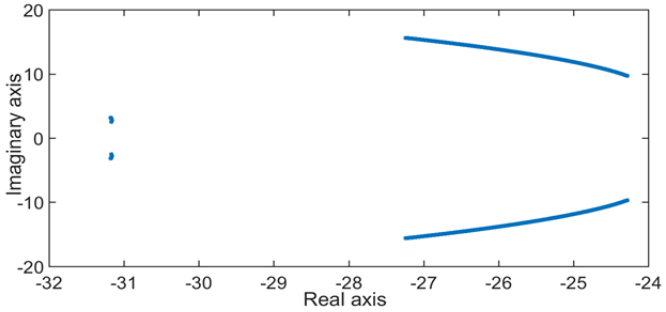

Fig. 12. Variation of eigenvalues with R_0 in S plane.

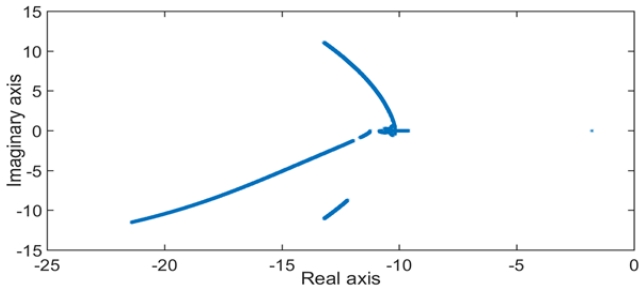

Fig. 13. Variation of eigenvalues with X_0 in S plane.

V. DROOP CONTROL OPTIMIZATION USING PSO

From the analysis given in Section IV, it is clear that the values of the parameters $k_p, k_q, k_{pv}, k_{ic}, R_0$ *and* X_0 decide the stability of the system. Hence the optimum values of the parameters are to be sought so that the system is stable. The objective of the optimization problem is to improve the stability of the system by controlling the position of eigenvalues. System will become stable when the eigenvalues are on the left side of imaginary axis and stability increases as the distance from imaginary axis increases.

Let eigenvalues be represented as $\lambda_i = Re_i + j\, Im_i$, where Re_i is the real part and Im_i is the imaginary part of the i^{th} eigenvalue. So the objective function is

Min J=maximum of (Re_i) such that $k_p, k_q, k_{pv}, k_{ic}, R_0$ *and* X_0 are within the limit.

In PSO, each particle is a real valued vector with dimension equal to the number of parameters to be optimized. Each particle is a solution to the optimization problem and such P particles will be there where P is the size of the population. Initially a random solution is taken with in the parameter limit which is nothing but position in the search space. The position of each particle is updated based on its inertia, personal best and group best according to the equation given below:

$$x_i(k+1) = x_i(k) + v_i(k+1) \quad (41)$$

$$v_i(k+1) = wv_i(k) + r_1C_1[P_i(k) - x_i(k)] + r_2C_2[g(k) - x_i(k)] \quad (42)$$

where,

$x_i(k)$: position of i^{th} particle in k^{th} iteration

$v_i(k)$: velocity of i^{th} particle in k^{th}iteration

w : inertia coefficient

C_1, C_2 : acceleration coefficient

$P_i(k)$: local best position of i^{th} particle in k^{th} iteration

$g(k)$: global best position among particles in k^{th} iteration

By conducting this updating process for velocity and position, at the end of a few iterations the optimum value is obtained. For the optimization problem discussed earlier, the parameters are given in Table 3.

By varying the microgrid control parameters X=$[k_p, k_q, k_{pv}, k_{ic}, R_0, X_0]$, the solution is obtained as X=[0.0045,5.32e-4,16.83,411.28,0.4,0.96] and J=-32.53. The convergence curve of objective function is given in Fig. 14.

The variations of dominant eigenvalues before and after optimization are given in Fig. 15 and 16. In Fig. 15, the real part of extreme right eigenvalue is at -0.012 and it is shifted to -32.53 after optimization as shown in Fig. 16.

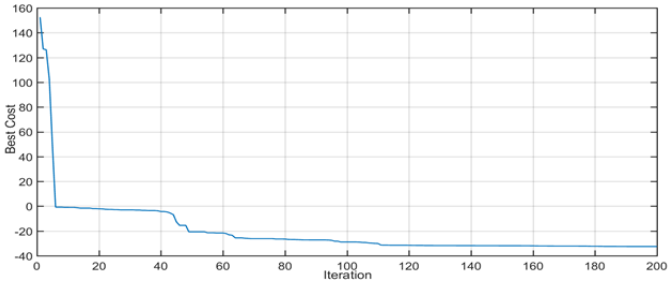

Fig. 14. Convergence curve of objective function.

TABLE III. PARAMETERS OF PSO

Parameter	**Values**
Number of iteration	200
Population size	50
Inertia coefficient	1
Damping ratio of inertia coefficient,	0.99
Individual acceleration coefficient, C_1	2
Global acceleration coefficient, C_2	2
Unknown variables	$[k_p, k_q, k_{pv}, k_{ic}, R_0, X_0]$
Lower limit of unknown variables	[1e-7, 1e-7,0,0,0,0]
Upper limit of unknown variables	[0.1,0.1,500,500,1,1]

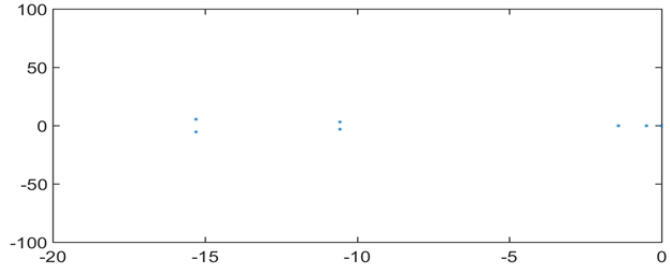

Fig. 15. Dominant eigenvalues before optimization in S plane.

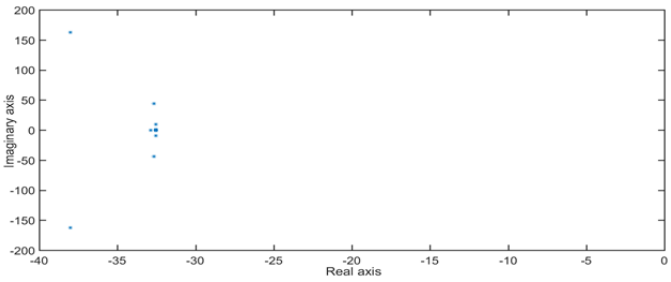

Fig. 16. Dominant eigenvalues after optimization in S plane.

Therefore, stability can be improved by the optimal setting of control parameters $k_p, k_q, k_{pv}, k_{ic}, R_0$ *and* X_0 .

VI. CONCLUSION

The small signal based state space model is used for analyzing the stability and dynamic performance of the microgrid system. From the eigenvalue analysis, it is observed that as k_p increases, the dominant eigenvalues move away from the real axis improving system performance while move closer to the imaginary axis deteriorating the stability. k_q has little influence on the dynamic performance of the system, but when the value is too large, the dominant roots move towards unstable region. The proportional parameter of voltage loop, k_{pv} and integral parameter of current loop, k_{ic} also have a great influence on the dominant eigenvalues whereas the integral parameters of voltage loop , k_{iv} and proportional parameter of current loop, k_{pc} do not affect the dominant roots significantly. The value of virtual impedance $Z_0 = R_0 + jX_0$, also affects the stability. Therefore the key parameters affecting the microgrid stability and dynamic performance are $k_p, k_q, k_{pv}, k_{ic}, R_0$ and X_0. By performing the particle swarm optimization, the optimum values of these parameters are found.

REFERENCES

[1] R. H. Lasseter and P. Piagi, "Providing premium power through distributed resources," in *Proc. IEEE 33rd Hawaii Int. Conf. System Sciences (HICSS'00)*, 2000, pp. 1–9.

[2] S. R. Wall, "Performance of inverter interfaced distributed generation," in Proc. *IEEE/PES-Transmission and Distribution Conf. Expo*., 2001, pp. 945–950.

[3] R. Lasseter, "Microgrids", Power Engineering Society Winter Meeting 2002. *IEEE*, vol. 1, pp. 305-308, 2002.

[4] P. Piagi and R. H. Lasseter, "Autonomous Control of Microgrids", *IEEE Power Engineering Society General Meeting*, pp. 8, 2006.

[5] J. A. P. Lopes, C. L. Moreira, and A. G. Madureira, "Defining Control Strategies for MicroGrids Islanded Operation", *IEEE Transactions on Power Systems*, vol. 21, pp. 916-924, 2006.

[6] K. De Brabandere, K. Vanthournout, J. Driesen, G. Deconinck, and R.Belmans, "Control of Microgrids", *IEEE Power Engineering Society General Meeting*, pp. 1-7, 2007.

[7] Daniel E. Olivares, A. Mehrizi-Sani, Amir H. Etemadi, "Trends in microgrid control", *IEEE Transactions on Smart Grid*, vol. 5, no. 4, pp. 1905-1919, 2014.

[8] P. Borazjani, N. I. A. Wahab, H. B. Hizam, A. Bt Che Soh, "A review on microgrid control techniques", Proc. *IEEE Innov. Smart Grid Technol. Asia (ISGT Asia)*, pp. 749-753, 2014.

[9] E. A. A. Coelho, P. C. Cortizo, and P. F. D. Garcia, "Small-signal stability for parallel-connected inverters in stand-alone AC supply systems," *IEEE Trans. Ind. App*l., vol. 38, no. 2, pp. 533–542, Mar./Apr. 2002.

[10] Y. Zhang, Z. Jiang, and X. Yu, "Small-signal modeling and analysis of parallel-connected voltage source inverters," in Proc. *IEEE 6th Int. Power Electron. Motion Control Conf*., May 2009, pp. 377–383.

[11] N. Pogaku, M. Prodanovic, and T. C. Green, "Modeling, analysis and testing of autonomous operation of an inverter-based microgrid," *IEEE Trans. Power Electron*., vol. 22, no. 2, pp. 613–625, Mar. 2007.

[12] K. Yu , Q. Ai , S. Wang , J. Ni , and T. Lv , " Analysis and optimization of droop controller for microgrid system based on small-signal dynamic model ," *IEEE Trans. Smart Grid* , vol. 7 , no. 2 , pp. 695 – 705 , Mar. 2016.

[13] Xiangyu Wu, Chen Shen and Reza Iravani, "Feasible range and optimum value of the virtual impedance for droop based control of microgrid" *IEEE Trans. Smart Grid* , vol. 8, no. 3, May 2017.